JOURNAL OF VIROLOGY, Mar. 1992, p. 1641–1648
0022-538X/92/031641-08$02.00/0

Vol. 66, No. 3

# Folding and Processing of the Capsid Protein Precursor P1 Is Kinetically Retarded in Neutralization Site 3B Mutants of Poliovirus

C. REYNOLDS,[1] D. BIRNBY,[2] AND M. CHOW[2]*

*Departments of Applied Biological Sciences[1] and Biology,[2] Massachusetts Institute of Technology, Cambridge, Massachusetts 02139-4307*

Received 2 August 1991/Accepted 9 December 1991

**Poliovirus mutants in neutralizing antigenic site 3B were constructed by replacing the glutamic acid residue at amino acid 74 of capsid protein VP2 (VP2074E), using site-specific mutagenesis methods. All viable mutants display small-plaque phenotypes. Characterization of these mutants indicates that capsid assembly is perturbed. Although the defect in capsid assembly reduces the yield of mutant virus particles per cell, the resultant assembled particle is wild-type-like in structure and infectivity. Analyses of capsid assembly intermediates show a transient accumulation of the unprocessed capsid protein precursor, P1, indicating that cleavage of the mutant P1 by the 3CD protease is retarded. The mutant VP0-VP3-VP1 complex generated upon P1 cleavage appears assembly competent, forming pentamer and empty capsid assembly intermediates and infectious virion particles. Although the structure of the infectious mutant virus is virtually identical with that of the wild-type virus, the thermal stability of the mutant virus is dramatically increased over that of the wild-type virus. Thus, mutations at this residue are pleiotropic, altering the kinetics of capsid assembly and generating a virus that is more thermostable and more resistant to neutralization by the site 3B monoclonal antibodies.**

The mature poliovirus virion is formed from 60 copies of the four capsid proteins VP1 (34 kDa), VP2 (30 kDa), VP3 (26 kDa), and VP4 (7.4 kDa). These proteins are arranged within an icosahedrally symmetric shell such that on the outer surface, VP1 proteins are located around each of the 12 fivefold rotational axes of symmetry and capsid proteins VP2 and VP3 are alternately positioned around each of the 20 threefold rotational axes. Assembly of this virus capsid is a complex multistep process involving the association of capsid protein subunits to form a series of assembly intermediates of defined stochiometries and architecture. Characterization of this morphogenic pathway is valuable for understanding the formation of neutralizing epitopes within an infected cell, for clarifying the molecular details of poliovirus pathogenesis, and for designing effective antiviral therapies and second-generation vaccines.

The capsid proteins are synthesized within the infected cell as a single translational unit, generating the 100-kDa capsid precursor (P1). Different stages of virion assembly are associated with specific cleavages of the capsid protein precursors. Thus, formation of pentamer intermediates appears to require cleavage of P1 to VP0-VP1-VP3, and in the final stages of virion assembly (conversion of the provirion to the mature virion), VP0 is cleaved to form capsid proteins VP4 and VP2 (18). A number of assembly intermediates have been identified in poliovirus-infected cells (18). These include the 5S uncleaved capsid precursor or protomer (P1), the 5S cleaved protomer (VP0-VP3-VP1), the 14S pentamer, the 73S native empty particle, and the provirion. The role of each intermediate within the assembly pathway and the molecular details affecting the formation of these intermediates are ill defined. Dissection of this pathway would be greatly facilitated by the availability of viral mutants defective in this assembly process. This report demonstrates that substitutions of the glutamic acid residue at VP2 amino acid residue 74 (VP2074E) generate viruses that are defective in the protein folding/capsid assembly pathway. Kinetic analyses of capsid assembly indicate that assembly of the mutant virus particle is delayed. This delay is due in part to a processing defect in these mutants such that cleavage of P1 is kinetically retarded. Interestingly, although the structural and biochemical analyses indicate that the fully assembled mutant particle is virtually identical to that of the wild-type particle, the infectivity of the mutant virus is more thermostable and resistant to 3B neutralizing monoclonal antibodies (MAbs).

## MATERIALS AND METHODS

**Cells and media.** HeLa cells in suspension culture were maintained in Joklik's modified minimal essential medium supplemented with 5% horse serum (GIBCO). HeLa or CV-1 cell monolayers were maintained in Dulbecco's modified Eagle's medium supplemented with 5 or 10% calf serum (Sigma), respectively. All dilutions of virus stocks were made in phosphate-buffered saline (PBS).

**Bacterial strains and plasmids.** *Escherichia coli* CJ236 (C. Joyce, Yale University) was used to generate phage stocks containing uridylated genomes. Phage stocks, phage replicative-form DNA, and all plasmids were grown in *E. coli* JM101. Plasmid pPVM1 contains an infectious cDNA copy of the poliovirus (serotype 1, Mahoney strain) genome originally obtained from P. Sarnow (University of Colorado Medical School, Denver) (20).

**Construction of mutants containing site-specific amino acid substitutions.** An M13 mp19 subclone was constructed by using unique *Aat*II and *Nhe*I sites in pPVM1, which contains sequences encoding the poliovirus VP2 capsid protein (nucleotides 1118 to 2470, nucleotide 1 being the 5′-terminal nucleotide of the viral genome). Synthetic deoxyoligonucleotides, corresponding to the region of the poliovirus genome between nucleotides 1159 and 1183, were synthesized with a random mixture of nucleotides at positions 1169, 1170, and

* Corresponding author.

1171 (Massachusetts Institute of Technology biopolymer facility), thus allowing all potential amino acid substitutions to occur at amino acid residue 74 of the VP2 capsid protein. The synthetic deoxyoligonucleotides were incorporated by the method of Kunkel (11). Amino acid substitutions were identified by dideoxynucleotide sequence analysis of individually recovered single-stranded phage genomes (19). Full-length poliovirus genomic cDNAs containing the amino acid substitutions of interest were generated by replacing the 1.3-kb *Aat*II-*Nhe*I wild-type fragment in plasmid pPVM1 with the identical fragment from the mutant subclone. The sequence of the entire P1 region within the constructed full-length mutant viral cDNA was determined to confirm the identity and location of the amino acid substitution and that this substitution was the only mutation within the capsid region of the infectious clone. Sequences of viable mutant viruses were determined by direct sequence analysis of the RNA genomes, using reverse transcriptase (16).

**DNA transfections and propagation of virus stocks.** Subconfluent (70 to 80%) HeLa or CV1 monolayers were transfected with 1 to 2 μg of plasmid pPVMI by using DEAE-dextran (15), overlaid with 1% agarose in Dulbecco's modified Eagle's medium–10% fetal calf serum, and incubated at 37°C. Virus isolates were recovered from the agar overlay after staining of the cell monolayer with 0.1% crystal violet.

Agar plugs from individual well-isolated plaques were transferred into 1 ml of PBS. Virus was released by three cycles of freezing and thawing. HeLa cell monolayers were infected with the plaque suspension at low multiplicity of infection (MOI; 0.005 to 0.01 PFU per cell) and incubated under liquid overlay. The cells and media were harvested when most cells displayed cytopathic changes. Virus was released from cells by three cycles of freezing and thawing. High-titer mutant stocks were prepared from HeLa suspension cells infected with virus from the low-MOI passage (MOI = 10 PFU per cell) (2). Cells were harvested 6 to 7 h postinfection (p.i.) and lysed, and the nuclei were removed by centrifugation. All biochemical data were obtained from cells infected with this high-titer stock.

**Single-step growth curve.** Suspension HeLa cells were infected with virus (MOI = 10). After 30 min of incubation at room temperature, cells were washed once in PBS, resuspended at $4 \times 10^6$ cells per ml, and incubated at 37°C. At various times, 100-μl aliquots were removed to monitor virus production. Virus was released by three freeze-thaw cycles and quantitated by plaque assay on HeLa cell monolayers.

**Viral RNA synthesis.** Suspension HeLa cells were infected with virus (MOI = 10). Actinomycin D (1 μg/μl) was added to cells 15 min p.i., and [$^{14}$C]uridine (0.5 μCi/ml, 350 mCi/mmol; NEN) was added 2 h p.i. At appropriate times, 100-μl aliquots were removed in triplicate and precipitated with 5% trichloroacetic acid (TCA)–1% $K_2HPO_4$–1% $K_4P_2O_7$. Precipitates were collected on glass fiber filters (Schleicher & Schuell) and counted in Beta-Fluor.

**Viral protein synthesis.** Infected HeLa cells (MOI = 5) were continuously labeled with [$^{35}$S]methionine (1,000 Ci/mmol; NEN) to a final concentration of 10 μCi/ml. Actinomycin D (1 μg/μl) was added 15 min p.i. [$^{35}$S]methionine was added to infected HeLa cell monolayers at 3 h p.i., and the cells were harvested at either 4, 5, or 6 h p.i. Cell lysates ($0.5 \times 10^7$ to $1 \times 10^7$ cells per ml) were prepared in RIPA buffer (10 mM Tris [pH 7.4], 150 mM NaCl, 1% deoxycholate, 1% Triton X-100, 0.1% sodium dodecyl sulfate [SDS]) and centrifuged at 4°C in a Ti40 rotor at 35,000 rpm for 30 min. Protein synthesis was quantitated in triplicate by trichloroacetic acid precipitation. The precipitates were collected on glass fiber filters and counted. Labeled viral proteins were examined by SDS-10% polyacrylamide gel electrophoresis (SDS-PAGE) and subsequent autoradiography (12, 13).

**Purified virus.** Virus was isolated on preformed CsCl gradients from infected cell lysates continuously labeled with [$^{35}$S]methionine. CsCl gradients in TNE (10 mM Tris [pH 7.5], 100 mM NaCl, 1 mM EDTA)–1% Brij 58–0.5% SDS (average density of 1.38 g/ml) were preformed in an SW40 rotor (38,000 rpm for 20 h). Gradients were fractionated from the bottom in 500-μl aliquots and counted. The concentration of virus particles was measured by optical density at 260 nm, using an extinction coefficient of 7.7 optical density units/mg/ml (18). Virus in TNE was titered by plaque assay (4).

**Protease sensitivity.** CsCl-purified virus was digested with bovine pancreas trypsin (tolylsulfonyl phenylalanyl chloromethy ketone TPCK treated; final concentration, 5 μg/ml); Sigma) or with *Staphylococus aureus* V8 (final concentration, 0.2 mg/ml) at room temperature for 60 min. Heated virus samples were first incubated at 50°C for 60 min prior to protease digestion. Virus capsid proteins were analyzed by SDS-PAGE.

**Thermal stability.** Thermal stability assays were performed as described previously (7). Virus ($10^7$ PFU/ml in 5 mM sodium phosphate [pH 7]) was incubated at 45°C. At various times, 10-μl aliquots were removed and the titer was determined by plaque assay on HeLa cell monolayers.

**Analysis of capsid assembly.** Pulse-chase studies were performed to analyze the kinetics of capsid assembly. Infected cells were labeled with [$^{35}$S]methionine (10 μCi/ml) for 30 min at 4 h p.i. And then a large excess of cold methionine (final concentration, 560 μg/ml) was added; cells were harvested at 4.5, 5, and 6 h p.i. Cells ($10^7$/ml) were lysed in TMN (10 mM Tris [pH 7.5], 10 mM NaCl, 1.5 mM $MgCl_2$)–1% deoxycholate–1% Brij 58–0.05 mM phenylmethylsulfonyl fluoride. Assembly intermediates were analyzed on sucrose gradients.

**Sucrose gradient analysis.** Mature infectious virus and empty capsid assembly intermediates were separated on 15 to 30% sucrose gradients prepared in TMN by centrifugation for 2.5 h at 39,000 rpm in an SW40 rotor at 4°C. Pentamer and monomer assembly intermediates were analyzed on 6 to 25% sucrose gradients in TMN after centrifugation for 16.5 h at 40,000 rpm in an SW40 rotor at 4°C. Fractions (300 μl) were collected and counted. Fractions were analyzed by SDS-PAGE.

**Mutant nomenclature.** Each of the mutants will be designated by the location of the mutation followed by the single-letter amino acid code of both the wild-type and mutant residue. By convention, amino acid residues 1 through 272 from VP2 are designated 2001 through 2272. Thus, mutation VP2074E.K is the substitution at VP2 amino acid residue 74 of the wild-type glutamic acid residue with lysine. To be consistent with the nomenclature used for other poliovirus mutants (1), the full name of VP2074E.K is 1C-VP2074E.K.

## RESULTS

Amino acid residue VP2074E is located on the surface of the native virus and contributes to neutralizing antigenic site 3B (16, 17). Although the glutamic acid side chain of VP2074E is apparently accessible to antibody-sized probes of 15 to 30 Å (1.5 to 3 nm) in diameter (unpublished data) and

```
                    Ala
                    Asp
                    Gly
* Lys               Leu
* Met               Tyr
   •                  •
-2071-2072Thr-Lys-2074Glu-Ser-2076-
                      •
                    Arg
                    Lys
```

FIG. 1. Amino acid substitutions within neutralization site 3B at residue 74 of capsid protein VP2 in poliovirus serotype 1, Mahoney strain. Mutations were constructed in the poliovirus expression vector pPVM1 (15) at the codon for VP2074E, using site-specific mutagenesis methods (11). Mutations above the linear sequence yield viable virus of small- to minute-plaque phenotypes. Mutations listed below the sequence are nonviable. *, Amino acid substitutions identified at VP2072T by sequence analysis of poliovirus mutants resistant to Sabin type-1 specific neutralizing MAbs (16).

mutations at VP2074E are potentially under antibody selection, examination of wild-type poliovirus sequences showed that the glutamic acid is conserved in all strains (17). Because residue VP2074E is close to the interface formed between two pentamer subunits during capsid assembly, the conservation of the glutamic acid suggests that this residue may play an important role during capsid assembly and that VP2074E mutants might be defective in this morphogenetic pathway.

**Construction and isolation of mutant viruses.** Amino acid substitutions at VP2074E were introduced by site-specific oligonucleotide mutagenesis methods. Seven amino acid substitutions were initially constructed and placed into the full-length cDNA poliovirus genome (Fig. 1). Viability of these mutant viral genomes was assessed by transfection of the mutated pPVM-1 plasmid into HeLa cell monolayers. Replacement of the glutamic acid residue with either lysine or arginine failed to yield viable virus. Subsequent replacement of the mutant lysine or arginine residue with the wild-type glutamic acid residue yields viable virus with wild-type plaque morphology and size. Thus, the nonviability of the lysine and arginine mutants was due not to technical artifacts introduced during the cloning and mutagenesis procedures but reflected the lethal phenotype of 2074E.K and 2074E.R mutations. Virus was recovered from HeLa cells transfected with a construct containing an aspartic acid substitution and surprisingly with constructs containing the nonpolar substitutions of a tyrosine, glycine, leucine, or alanine residue for the VP2074E residue. Sequence analysis of the entire P1 region from the cDNA clone and the VP2 region from the RNA genomes of viable mutants confirmed the amino acid substitutions at VP2074E and identified these substitutions as the sole amino acid changes. The mutants showed no temperature sensitivity for growth at 33 versus 39°C and no host range dependence, appearing to grow equally well in HeLa and CV-1 cells (data not shown).

Plaque assays of the low-MOI passage virus stocks revealed that all mutant viruses grew to titers that were approximately 10-fold lower than that typically observed for transfection-derived wild-type stocks. In addition, the time required to observe complete cytopathology varied among mutant viruses and was always at least a day later than for wild-type virus. Finally, all VP2074E mutants (including the aspartic acid mutant) displayed a small- to minute-plaque phenotype (Fig. 2). To investigate the nature of this small-

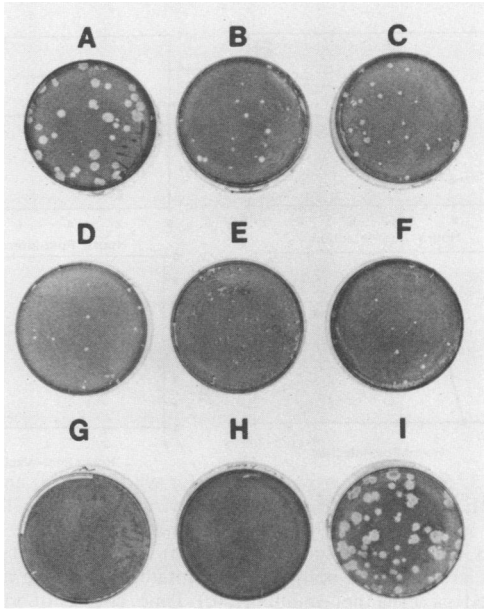


FIG. 2. Plaque phenotypes of poliovirus VP2074E mutants. HeLa cell monolayers were infected with the viable transfection-derived plaque isolates of mutant viruses (A to F). Monolayers were incubated for 48 h at 37°C and stained with crystal violet. The wild-type and mutant codons are given below in parentheses. For the nonviable mutants (G and H), the plates after transfection of the mutant cDNA are shown. These plates were harvested 5 days posttransfection. (A) VP2074E (wild type, gag); (B) VP2074E.A (gct); (C) VP2074E.D (gac); (D) VP2074E.G (ggc); (E) VP2074E.L (ctt); (F) VP2074E.Y (tac); (G) VP2074E.R (cga); (H) VP2074E.K (aaa); (I) VP2074E.K.E (gag→aaa→gaa).

plaque phenotype, the biological properties of the mutants were characterized further.

**Characterization of VP2074E mutants.** Substitutions of the glutamate residue with a nonpolar residue (tyrosine, glycine, leucine, or alanine) yielded VP2074E mutants with similar biological properties. The aspartic acid substitution, VP2074E.D, displayed phenotypes intermediate between those of the wild type and the nonpolar substituted VP2074E mutants.

The replication efficiencies of VP2074E mutants were examined in one-step growth experiments (Fig. 3a and b). Virus production in the VP2074E.A and -E.L mutants appeared delayed by approximately 1 h but, like the wild-type infection, reached maximum levels between 5 and 6 h p.i. The maximum yield of infectious virus per cell was 10-fold less than that of wild-type virus. Identical results were obtained with the other mutants with nonpolar substitutions at this position. The growth kinetics in the VP2074E.D mutant-infected cells were indistinguishable from those of the wild-type-infected cells (data not shown).

The kinetics of RNA synthesis were identical for the wild-type and all mutant viruses. Maximal rates of RNA synthesis in infected cells occurred between 4 and 5 h p.i., and the total amounts of RNA synthesized were similar (Fig. 3c). Examination of the labeled RNA products on 1% agarose gels showed the expected genomic-length RNA (data not shown). Consistent with the kinetics of RNA synthesis, the kinetics of protein synthesis in mutant- and wild-type-infected cells were identical (Fig. 3d). Thus, the delay in virus production observed in the single-step growth studies was not due to defects in virus-receptor recognition, virus binding, or virus uncoating.

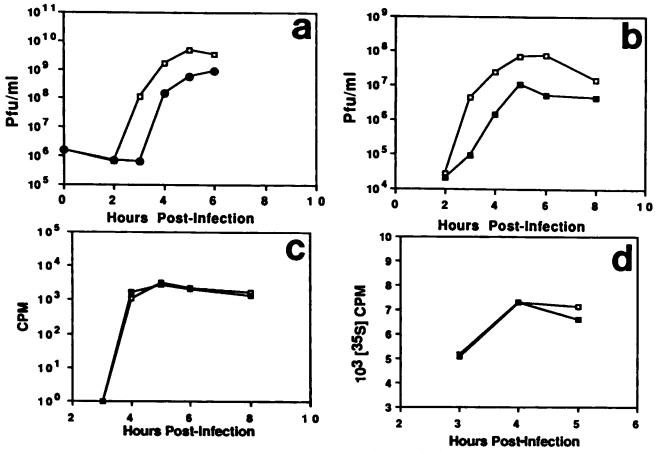


FIG. 3. Single-step growth curves for wild-type (□) and mutant (VP2074E.A [●] and VP2074E.L [■]) viruses. HeLa cells in suspension were infected (MOI = 10), and aliquots were taken at specified times postinfection. (a and b) Total yield of infective particles at each time point was quantitated by plaque assay and expressed as PFU per milliliter. (c) Time course of viral RNA synthesis was measured by [$^{14}$C]uridine incorporation and expressed as counts per minute. (d) Protein synthesis was quantitated by trichloroacetic acid precipitation of [$^{35}$S]methionine-labeled virus-infected cells.

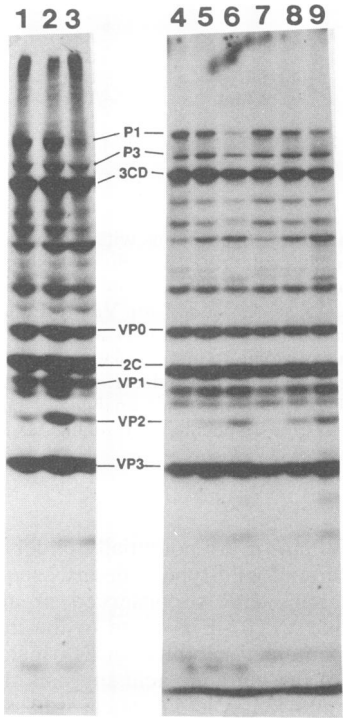


FIG. 4. [$^{35}$S]methionine labeling of wild-type- and mutant-infected cells. Wild-type (lanes 1 to 3)-, VP2074E.G (lanes 4 to 6)-, and VP2074E.Y (lanes 7 to 9)-infected HeLa cell monolayers were continuously labeled from 3 h p.i. ([$^{35}$S]methionine; 10 μCi/ml, 1,000 Ci/mmol). Lysates were prepared from infected cells at 4 (lanes 1, 4, and 7), 5 (lanes 2, 5, and 8), and 6 (lanes 3, 6, and 9) h p.i. and separated by 10% SDS-PAGE.

The profiles of synthesized proteins were examined in mutant- and wild-type-infected cell lysates continuously labeled with [$^{35}$S]methionine (Fig. 4). All viral proteins except capsid protein VP2 were observed to have normal stoichiometries. Thus, overall viral protein synthesis and shutdown of host protein synthesis appeared unaffected in these mutants. In wild-type-infected cells, appreciable amounts of VP2 were observed normally at 4 h p.i. and continued to accumulate until cells began to lyse (at 6 to 6.5 h p.i.). Thus, the apparent lower concentration of VP2 (and other viral proteins) at 6 p.i. is artifactual and due to release of viral proteins into the culture media as cells lyse. At 4 h p.i., VP0 concentrations appeared normal in the VP2074E.L, -E.A, -E.Y, and -E.G mutant-infected cells, but VP2 appeared to be absent (Fig. 4, lanes 4 and 7). As infection proceeded, labeled VP2 accumulated in these mutant-infected cell lysates but never achieved wild-type levels (Fig. 4, lanes 4 to 9). Trace amounts of VP2 were observed in VP2074E.D-infected cells at 4 h p.i., and by 5 h p.i., the amounts approached wild-type levels (data not shown). Because protein synthesis appeared normal and processing of VP0 to VP4 and VP2 occurs during capsid assembly, virion assembly appears altered in the VP2074E mutants.

**Structure of mutant virus particles.** The reduced virus titers from the single-step growth experiments and delayed appearance of VP2 in the cell lysates suggested that capsid assembly could be defective, producing a mutant virus particle with altered capsid protein composition (i.e., increased amounts of VP0) or a particle with normal capsid protein composition but with reduced infectivity. Therefore, the structures and conformational architectures of the mutant virions were characterized by using different biochemical and biological probes. Like the wild-type virus, all mutant viruses banded in isopycnic CsCl density gradients at a density of 1.35 mg/ml, had a sedimentation value of 150S in sucrose gradients, and were resistant to detergent and high ionic strength (data not shown). The protein compositions of the mutant viruses were examined after isolation from CsCl density gradients (Fig. 5, lanes 1 and 5). The wild-type particle contains VP1, VP2, VP3, VP4, and approximately one copy of VP0 per particle. The protein compositions of all mutant viruses were identical to that of the wild type. Finally, the specific infectivities of all mutant viruses were approximately 100 particles per PFU, similar to that of the wild-type virus (data not shown).

The overall conformational similarity of the mutant and wild-type viruses is suggested by the sensitivity of the mutant viruses to neutralization by the Sabin MAbs that specifically recognize neutralization site 2 (MAbs 2 to 8) and their insensitivity to protease digestion. Consistent with these residues contributing to neutralization site 3B, most VP2074E mutants were partially or completely resistant to neutralization by one or more of the MAbs that recognize site 3B (MAbs 10, 13, and 15) (Fig. 6). Differences in the neutralization patterns with individual 3B MAbs likely reflect differences in the specific interactions of the MAb with the substituted residue. The mutants are neutralized by all site 2 MAbs tested. Neutralization site 2 is a conformationally complex site formed by the juxtaposition of two loops: VP1220-VP1226 and VP2160-VP2172 (16). The ability of all site 2 MAbs to recognize and subsequently neutralize the VP2074E mutants indicates that the surface conformations surrounding this site were unaltered. The resistance of the mutants (constructed in a Mahoney strain background) to Sabin 1 site 3A MAbs (MABs 1, 9, 11, and 12) is due to specific sequence differences observed between Sabin 1 and Mahoney strains at this site (6). The conformational integrity of the mutant virions is more stringently tested by their

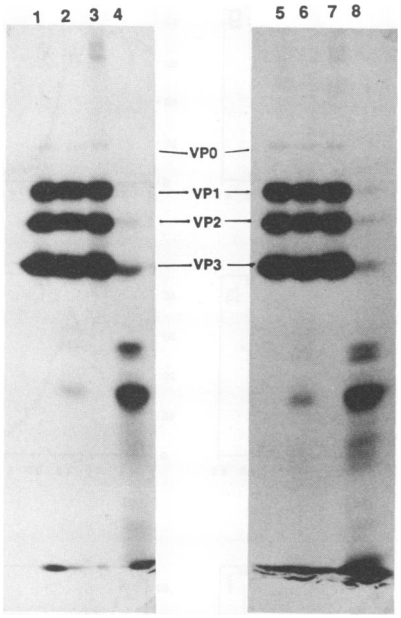


FIG. 5. Trypsin sensitivity of wild-type and mutant poliovirus. Band purified, [$^{35}$S]methionine-labeled virus samples were either unheated (lanes 1, 2, 5, and 6) or heat at 50°C for 60 min (lanes 3, 4, 7, and 8). Samples (lanes 2, 4, 6, and 8) were digested with trypsin (5 μg/ml) for 60 min at room temperature, and the products were separated by 10% SDS-PAGE. Lanes: 1 to 4, wild type; 5 to 8, VP2074E.G.

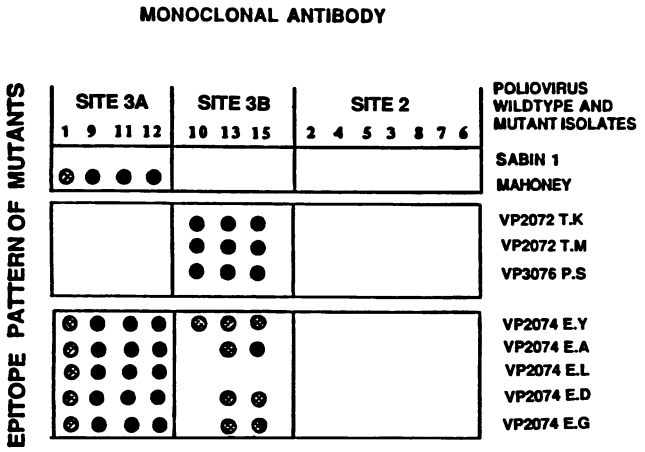


FIG. 6. Antibody resistance patterns of VP2074E viral mutants. Mutants were tested in cross-neutralization assays for ability to lyse HeLa cell monolayers in the presence of a neutralizing MAb (16). Neutralization resistance or escape by the viral mutant is defined by lysis of cell monolayers in the presence of neutralization titers 10-fold higher than that required to neutralize the wild-type parent. Partial resistance is defined by lysis of cell monolayers in the presence of 4- to 8-fold but not 10-fold excess neutralizing antibody titers. Individual neutralization is indicated by the absence of a circle, resistance is indicated by ●, and partial resistance is indicated by ◍. VP2072T and VP3076P mutants were identified previously by sequence analysis of neutralization-resistant variants (16). VP2074E mutants were generated by site-specific mutagenesis.

sensitivity to trypsin and *S. aureus* V8 protease digestion. Mature wild-type virus is resistant to cleavage by these enzymes, whereas other forms of the wild-type virus particle (including the provirion and heated virus) are highly sensitive to proteolytic digestion. All mutant virions were resistant to trypsin cleavage (Fig. 5). Moreover, identical trypsin cleavage patterns were observed for wild-type and mutant heated-treated viruses. Thus, the overall conformational rearrangements that occur upon heat treatment of the virus particle and that lead to exposure of specific enzyme-sensitive sites appeared identical. Similar results were observed with use of *S. aureus* V8 protease (data not shown). Finally, the infectious VP2074E.Y virus particle can be crystallized in a form which is nearly isomorphous with that of the wild-type virus. Difference maps reveal no major structural changes other than the expected mutation (9a). These data indicate that the structures of the infectious particle for these VP2074E mutants appear virtually identical to that of the wild-type virus.

The mutant viruses were indistinguishable from the wild-type virus for all parameters studied except behavior upon heating (Fig. 7). The infectivity of the wild-type virus is very thermolabile upon heating at 45°C. However, substitution of the VP2074E residue with nonpolar amino acids substantially increases the thermal stability of the virus. Interestingly, even the conservative substitution of the glutamic acid with an aspartic acid results in a stability phenotype that is intermediate between those of the wild-type virus and the mutants with hydrophobic substitutions at VP2074E. Thus, all substitutions tested at VP2074E appear to stabilize infectivity of the virion particle.

**Kinetics of capsid assembly.** The normal capsid structure and specific infectivity of the mutant virions suggested that the delayed appearance of VP2 in cell lysates may reflect delays or alterations in the kinetics of capsid assembly, which lead to an overall reduction in particle yield from mutant-infected cells. The kinetics of capsid assembly were examined in VP2074E.L mutant- and wild-type-infected cell lysates which were labeled with [$^{35}$S]methionine for 30 min and subsequently chased with excess methionine. Capsid intermediates were examined on sucrose density gradients (Fig. 8). As expected, in wild-type-infected cells at the end of the labeling period, the majority of the label is in the 5S protomer and 14S pentamer intermediates, with a small amount of label sedimenting as the mature 150S particle and a fast-sedimenting fraction (Fig. 8a and g). By SDS-PAGE analyses, this fast-sedimenting fraction appears due to nonspecific aggregates of mature virion particles and assembly intermediates. Within the first hour of the chase, the major-

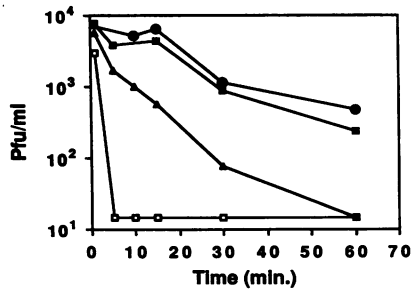


FIG. 7. Stability of VP2074E poliovirus mutants to thermoinactivation. Virus diluted to $10^6$/ml with 5 mM phosphate buffer (pH 7.0) was incubated in a 45°C water bath in completely submerged, close-capped Eppendorf tubes. Aliquots were periodically removed, and the titer of infectious virus remaining was measured by plaque assay. Symbols: □, wild type; ●, VP2074E.A; ▲, VP2074E.D; ■, VP2074E.L.

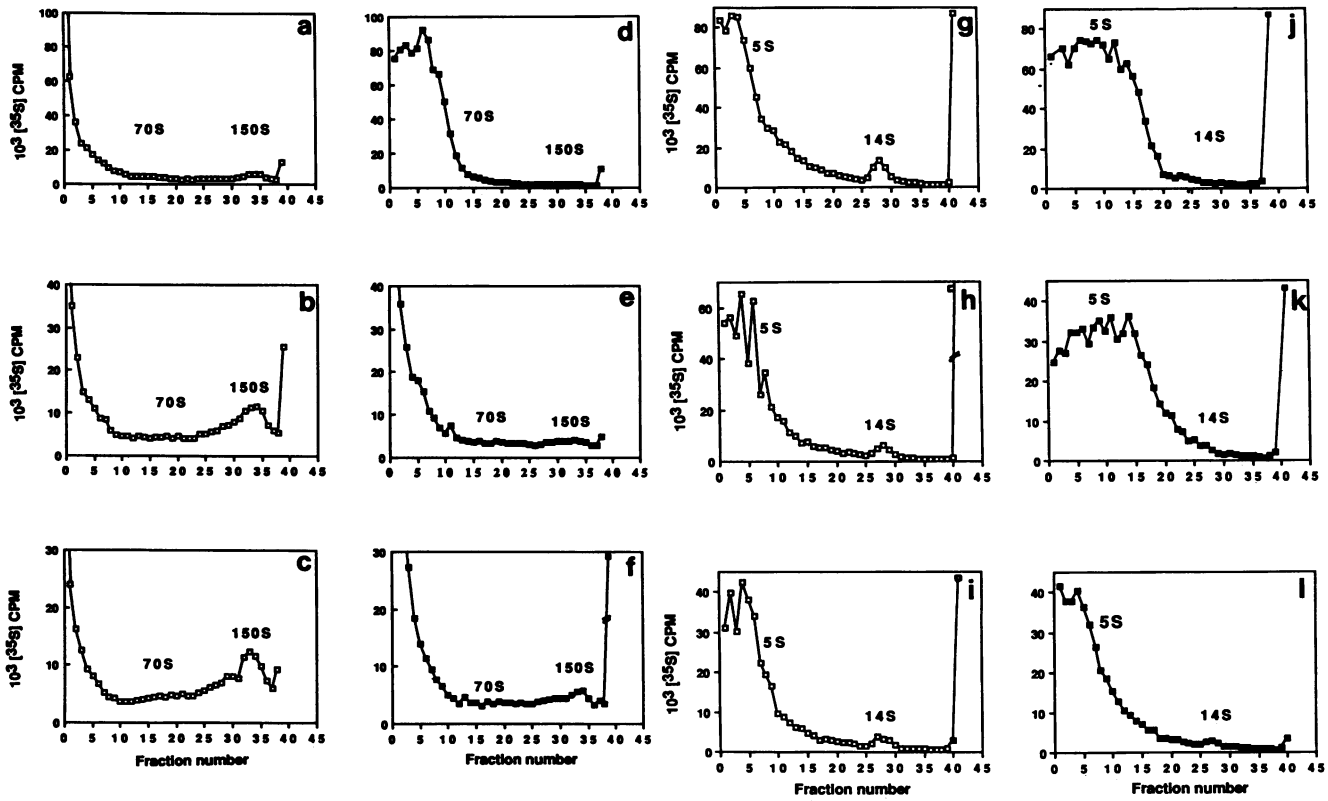


FIG. 8. Sucrose gradient analysis of capsid assembly kinetics. HeLa cells infected with the wild type (□) and VP2074E.L (■) were labeled at 4 h p.i. with [$^{35}$S]methionine (1 mCi/liter, 1,000 Ci/mmol). Excess unlabeled methionine (560 μM, final concentration) was added at 4.5 h p.i. Aliquots ($8 \times 10^6$ cells) were removed at 4.5, 5, and 6 h p.i., and cell lysates were prepared in TMN lysis buffer. Lysates from equivalent numbers of infected cells were sedimented in 15 to 30% (a to f) and 6 to 25% (g to l) linear sucrose gradients. Fractions (300 μl) were collected from the top of the gradient. Sedimentation profiles of the assembly intermediates at 4.5 (a, d, g, and j), 5 (b, e, h, and k), and 6 (c, f, i, and l) h p.i. are shown.

ity of label in the 5S, 14S, and 70S wild-type intermediates moves into the 150S peak (Fig. 8b and c). In contrast, in VP2074E.L mutant-infected cells at the end of the labeling period, virtually no label is observed sedimenting as a 150S particle; the majority of label is in the 5S protomer peak (Fig. 8d and j). During the chase period, the 5S label moves into the 150S peak, but with slower kinetics than that observed in wild-type-infected cells (Fig. 8e and f). The slower kinetics of virion formation in mutant-infected cells appears to correlate with movement of label out of the 5S protomer fractions (Fig. 8k and l). Because overall recovery of label was identical in both wild-type and mutant sucrose gradients, the slower accumulation of label sedimenting at 150S and the transient accumulation of labeled 5S protomers reflect a difference in the kinetics of virion formation between wild-type and VP2074E mutants. Examination of the unfractionated cell lysates and of 5S and 150S fractions by SDS-PAGE confirms that unassembled labeled cleaved (VP0-VP3-VP1) and uncleaved (P1) protomers are chased into mature virion particles (Fig. 9). P1 and 1ABC (VP0-VP3) proteins were identified on the basis of their molecular weights and antibody reactivities in Western immunoblots (data not shown). The slower movement of label from the 5S peak to other assembly intermediates may be due to slower processing of the uncleaved protomer (P1) to the cleaved protomer (VP0-VP3-VP1), or it may be due to slower pentamer formation from the cleaved protomer. Analyses of the 5S mutant and wild-type fractions reveal that higher levels of

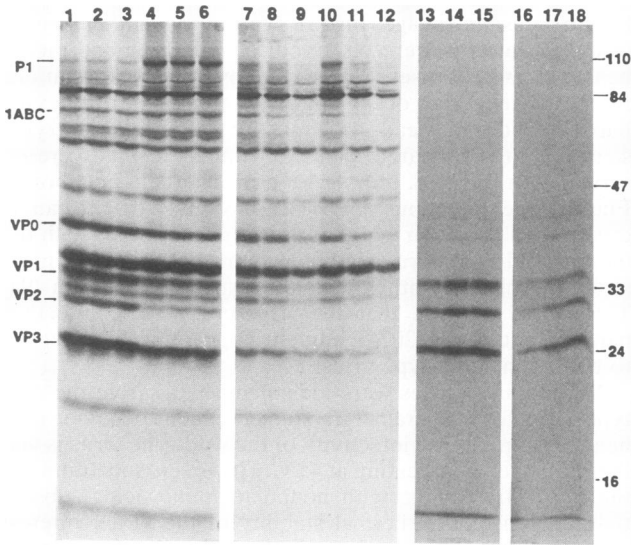


FIG. 9. Gel analysis of the unfractionated cell lysates and of the 5S and 150S fractions from sucrose gradients of capsid assembly intermediates. Shown are results for unfractionated cell lysates of wild-type (lanes 1 to 3) and VP2074E.L (lanes 4 to 6) fractions, the 5S region from sucrose gradients of wild-type lysates (lanes 7 to 9) and VP2074E.L lysates (lanes 10 to 12), and the 150S region from sucrose gradients of wild-type (lanes 13 to 15) and VP2074E.L (lanes 16 to 18). Lysates are from infected cells harvested at 4.5 (lanes 1, 4, 7, 10, 13, and 16), 5 (lanes 2, 5, 8, 11, 14, and 17), 6 (lanes 3, 6, 9, 12, 15, and 18) h p.i.

the uncleaved P1 are present in the VP2074E.L mutant 5S fraction (Fig. 9, lanes 10 and 11). However, after a 90-min chase period, the levels of P1 in mutant 5S fractions are comparable to those observed in the wild-type 5S fractions (Fig. 9, lane 12). Thus, processing of P1 to the cleaved protomer VP0-VP3-VP1 appears retarded in these mutants, leading to a transient accumulation of P1. Protein bands corresponding to the cleaved protomer (VP0-VP3-VP1) and to the processing intermediate (1ABC-VP1) are observed in the 5S fractions from wild-type- and mutant-infected cell lysates at the end of the 30-min labeling period; however, lower levels of the cleaved protomer and 1ABC are observed in the mutant-infected 5S fractions. Label in mutant 1ABC and the cleaved protomer is also chased to higher-order assembly structures (pentamer, empty capsid, and virion). Thus, the mutant P1 observed in the mutant lysates is assembly competent but assembled into virions with kinetics slower than that of the wild-type virus.

## DISCUSSION

All substitutions of the glutamic acid residue at VP2 amino acid 74 (VP2074E) had deleterious effects on virus growth. In all viable mutant VP2074E viruses, the proteolytic processing of the capsid protein precursor P1 to form VP0-VP3-VP1 appears retarded. However, upon cleavage of P1, these mutants appear to assemble a normal infectious capsid. Consequently, the delayed cleavage of P1 contributes to the approximately 10-fold-lower yield of infectious virus per cell in these viable mutants than in wild-type virus and to the small-plaque phenotype of these mutants. Nonviable mutants were obtained when glutamic acid was substituted with lysine or arginine, amino acids with positively charged side chains. Although these mutants were not characterized further, on the basis of the phenotypes of the viable mutants, it is likely that in these nonviable mutants, P1 processing and virion assembly are also defective.

The retarded processing of P1 contributes to the delayed appearance of infectious virus in a single round of infection and to the overall smaller burst size. However, observable amounts of VP0 appear present in continuously labeled mutant infected cell lysates at 5 and 6 h p.i. which are apparently not efficiently assembled into mature VP2-containing virions (16a). This finding suggests that there may additional defects at later stages of virion assembly. Several types of poliovirus mutants have been described in which the late stages of capsid assembly are affected. An in-frame insertion of six amino acids containing an alternate Q-G cleavage has been placed at the VP3-VP1 junction (3). Cleavage of the VP3-VP1 junction occurs in this mutant almost exclusively at this alternate Q-G site. This mutant displays a temperature-sensitive defect in VP0 cleavage into VP4-VP2 at 39°C, and a significant amount of the uncleaved VP0 accumulates in sucrose fractions containing mature virions. It is unclear whether the infectious mature virions contain increased amounts of VP0 or the increased uncleaved VP0 is present as part of a provirion structure that is accumulating also in these fractions at 39°C. A mutant has also been isolated that has an in-frame deletion at the VP3-VP1 junction of the amino-terminal four residues in VP1 and alters the Q-G cleavage site to Q-M. The observed molecular weights of VP3 and VP1 suggest that cleavage of VP3 and VP1 occurs at the Q-M bond (10). RNA packaging appears retarded in this mutant. Finally, intriguingly, a mutant containing a point mutation in VP2 (VP2076R.E) at the nonpermissive temperature (39°C) interferes with VP0 cleavage and accumulates provirions (5). Although the VP2074E mutants described here do not appear to be temperature sensitive, the accumulation of provirions in the VP2076R.E mutant suggests that the VP2074E mutants might be similarly affected at this stage of virion assembly. Although the occurrence of late assembly defects remain to be defined for the VP2074E mutants, because labeled 5S protomers can be chased into mature 150S virions, we anticipate that these defects will also likely be kinetic in character.

In contrast to these other mutants, the VP2074E mutants appear defective also at the initial stages of virion assembly, during folding and processing of P1. Thus, they allow dissection of these early stages. P1 processing is efficiently achieved by the viral 3CD protease, which cleaves the Q-G sequence at the VP2-VP3 and VP3-VP1 boundaries (21). The recognition of these cleavage sites appears dependent in some unknown manner on the secondary and tertiary structure of the P1 protein (22). Because the sequences surrounding both cleavage sites are unaltered, the molecular weights of the mutant VP1, VP2, VP3, and VP4 appear to be identical with that of wild type, and the structures of the assembled virions for each mutant reveal no major differences from that of the wild-type parent, cleavage of the mutant P1 by the 3CD protease appears to occur at the correct Q-G sites. Thus, the mutant P1 protomer appears to fold correctly into the secondary and tertiary structures necessary for 3CD recognition and cleavage. This suggests that the observed slower kinetics of P1 processing in these VP2074E mutants may be due to the slower folding kinetics of the mutant P1 protein. Once P1 is correctly folded, processing by the 3CD protease can occur.

The products of a partially cleaved protomer (1ABC and VP1) are visible in both wild-type and mutant 5S fractions. It has been questioned whether the two Q-G cleavages necessary to generate the cleaved protomer occurred in a specific order. The clear presence of 1ABC and VP1 proteins and the absence of the potentially alternative 1CD cleavage intermediate (formed by VP3-VP1 sequences) indicate that the sequence of P1 cleavages by 3CD is not random but is ordered. Thus, the Q-G bond at the VP3-VP1 junction is cleaved first, followed by cleavage of the Q-G bond at the VP2-VP3 junction. The orderliness of these cleavages suggests that a conformational or structural transition may be linked with cleavage of the first Q-G bond to enable 3CD recognition and cleavage of the second Q-G bond. Within wild-type lysates, P1 processing is normally very efficient such that the major labeled species present in the 5S fractions is usually the completely cleaved protomer (VP0-VP3-VP1), with labeled P1 and 1ABC proteins being barely discernible by SDS-PAGE analyses. This suggests that in wild-type-infected cells, the assembly of pentamers from the cleaved protomer is the rate-limiting step in pentamer formation. The predominance of P1 and concomitant lower levels of 1ABC-VP1 and cleaved protomer (VP0-VP3-VP1) in mutant 5S fractions suggest that P1 folding and the initial processing step may be sufficiently inhibited that it becomes the rate-limiting step for pentamer formation in VP2074E mutants.

Although the VP2074E mutant particle is virtually indistinguishable in structure from the wild-type virus, its infectivity is more thermostable than that of the wild type, exhibiting a 10-fold increase in thermal stability upon incubation at 45°C. Even the conservative aspartic acid substitution displays a stability that is intermediate between those of the wild type and the other VP2074E mutants. Thus, the

identity of the amino acid at this residue position appears to affect the thermal stability of the viral particle. This is surprising because the glutamic acid side chain within the virus particle does not appear to be structurally interacting with any other residues and appears to extend into solvent space. Temperature-sensitive mutants were previously isolated for their ability to grow at 39°C (8, 14). Those that have been characterized to date are located in four regions: (i) the protomer interfaces within a pentamer; (ii) the hydrocarbon-binding pocket of VP1; (iii) an assembly-dependent seven-stranded beta sheet at threefold axes; and (iv) the amino terminus of VP1. Although VP2074E is not located in the interface of fivefold related protomers, it is at the interface between two pentamers. It is possible that the thermal stability observed in these mutants is due to altered interactions at pentamer interfaces. The details remain to be studied.

Mutations at the VP2074E site display pleiotropic effects, affecting the capsid assembly pathway, the thermal stability of the assembled capsid, and neutralization resistance to the site 3B MAbs. The structural information provided by the location of this glutamic residue within the atomic structure does not provide any insight at this juncture as to mechanisms that account for the increased thermal stability or for the slower kinetics of capsid assembly. However, it is interesting that several mutations in different regions of the capsid proteins with unexpected pleiotropic effects have been described (10, 15). Thus, the generation of pleiotropic phenotypes may occur at unexpected greater frequencies by substitution of an amino acid residue within the virus capsid. This may reflect the multiple functional and structural roles that the capsid proteins must play at different stages of the virus life cycle. Thus, the amino acid residues present in capsid protein sequences of wild-type viruses may represent the best compromise of allowed residues that satisfy these disparate roles during viral infection.

## ACKNOWLEDGMENTS

We thank Anne Mosser for the gift of the MAbs, James Hogle for helpful discussion, Aline Cornelius for assistance in manuscript preparation, and Keith Thornton for excellent technical assistance.

This work was supported by Public Health Service grant AI122627 from the National Institutes of Health.

## REFERENCES

1. **Bernstein, H. D., P. Sarnow, and D. Baltimore.** 1986. Genetic complementation among poliovirus mutants derived from an infectious cDNA clone. J. Virol. **60:**1040–1049.
2. **Bernstein, H. D., N. Sonenberg, and D. Baltimore.** 1985. Poliovirus mutant that does not selectively inhibit host cell protein synthesis. Mol. Cell. Biol. **5:**2913–2923.
3. **Blair, W. S., S.-S. Hwang, M. F. Ypma-Wong, and B. L. Semler.** 1990. A mutant poliovirus containing a novel proteolytic cleavage site in VP3 is altered in viral maturation. J. Virol. **64:**1784–1793.
4. **Chow, M., and D. Baltimore.** 1982. Isolated poliovirus capsid protein VP1 induces a neutralizing response in rats. Proc. Natl. Acad. Sci. USA **79:**7518–7521.
5. **Compton, S. R., B. Nelsen, and K. Kirkegaard.** 1990. Temperature-sensitive poliovirus mutant fails to cleave VP0 and accumulates provirions. J. Virol. **64:**4067–4075.
6. **Diamond, D. C., B. A. Jameson, J. Brown, M. Kohara, S. Abe, H. Itoh, T. Komatsu, M. Arita, S. Kuge, A. D. M. E. Osterhaus, R. Crainic, A. Nomoto, and E. Wimmer.** 1985. Antigenic variation and resistance to neutralization in poliovirus type 1. Science **229:**1090–1093.
7. **Dorval, B. L., M. Chow, and A. M. Klibanov.** 1989. Stabilization of poliovirus against heat inactivation. Biochem. Biophys. Res. Commun. **159:**1177.
8. **Filman, D. J., R. Syed, M. Chow, A. J. Macadam, P. D. Minor, and J. M. Hogle.** 1989. Structural factors that control conformational transitions and serotype specificity in type 3 poliovirus. EMBO J. **8:**1567–1579.
9. **Hogle, J. M., M. Chow, and D. J. Filman.** 1985. Three dimensional structure of poliovirus at 2.9 Å resolution. Science **229:**1358–1365.

9a. **Jacobson, D., and J. Hogle.** Personal communication.

10. **Kirkegaard, K.** 1990. Mutations in VP1 of poliovirus specifically affect both encapsidation and release of viral RNA. J. Virol. **64:**195–206.
11. **Kunkel, T.** 1985. Rapid and efficient site-specific mutagenesis without phenotypic selection. Proc. Natl. Acad. Sci. USA **82:**488–492.
12. **Laemmli, U. K.** 1970. Cleavage of structural proteins during the assembly of the head of bacteriophage T4. Nature (London) **227:**680–685.
13. **Laskey, R. A.** 1980. The use of intensifying screens or organic scintillators for visualizing radioactive molecules resolved by gel electrophoresis. Methods Enzymol. **65:**363–371.
14. **Minor, P. D., G. Dunn, D. M. A. Evans, D. I. Magrath, A. John, J. Howlett, A. Phillips, G. Westrop, K. Wareham, J. W. Almond, and J. M. Hogle.** 1989. The temperature sensitivity of the Sabin type 3 vaccine strain of poliovirus: molecular and structural effects of a mutation in the capsid protein VP3. J. Gen. Virol. **70:**1117–1123.
15. **Moscufo, N., J. Simons, and M. Chow.** 1991. Myristoylation is important at multiple stages in poliovirus assembly. J. Virol. **65:**2372–2380.
16. **Page, G. S., A. G. Mosser, J. M. Hogle, D. J. Filman, R. R. Rueckert, and M. Chow.** 1988. Three-dimensional structure of the poliovirus serotype 1 neutralizing determinants. J. Virol. **62:**1781–1794.

16a. **Reynolds, C., and M. Chow.** Unpublished data.

17. **Reynolds, C., G. Page, H. Zhou, and M. Chow.** 1991. Identification of residues in VP2 that contribute to poliovirus neutralization antigenic site 3B. Virology **184:**391–396.
18. **Rueckert, R. R.** 1985. Picornaviruses and their replication, p. 705–738. *In* B. Fields (ed.), Virology. Raven Press, New York.
19. **Sanger, F., S. Nicklen, and A. R. Coulsen.** 1977. DNA sequencing with chain-terminating inhibitors. Proc. Natl. Acad. Sci. USA **74:**5463–5467.
20. **Sarnow, P.** 1989. Role of 3′-end sequences in infectivity of poliovirus transcripts made in vitro. J. Virol. **63:**467–470.
21. **Ypma-Wong, M. F., P. G. Dewalt, V. H. Johnson, J. G. Lamb, and B. L. Semler.** 1988. Protein 3CD is the major poliovirus proteinase responsible for cleavage of the P1 precursor. Virology **166:**265–270.
22. **Ypma-Wong, M. F., D. J. Filman, J. M. Hogle, and B. L. Semler.** 1988. Structural domains of the poliovirus polyprotein are major determinants for proteolytic cleavage at gln-gly pairs. J. Biol. Chem. **263:**17846–17856.